TRENDS IN SCIENCES 2026; 23(3): 12119
https://doi.org/10.48048/tis.2026.12119 RESEARCH ARTICLE

Molecular Identification of *Spirogyra* Species Using *rbc*L Markers and Their Chemical Compositions

Nopparut Sitthiwong[1], Kaewkanlaya Sotthisawad[1], Supakorn Arthan[2,*], Jeeraporn Pekkoh[3] and Kittiya Phinyo[4]

[1]*Program of Biology, Faculty of Science and Technology, Sakon Nakhon Rajabhat University, Sakon Nakhon 47000, Thailand*
[2]*Program of Chemistry, Faculty of Science and Technology, Sakon Nakhon Rajabhat University, Sakon Nakhon 47000, Thailand*
[3]*Department of Biology, Faculty of Science, Chiang Mai University, Chiang Mai 50200, Thailand*
[4]*Office of Research Administration, Chiang Mai University, Chiang Mai 50200, Thailand*

([*]Corresponding author's e-mail: supakorn.a@snru.ac.th)

Received: 30 September 2025, Revised: 8 October 2025, Accepted: 15 October 2025, Published: 20 December 2025

Abstract

Spirogyra are green algae that occur widespread in freshwater habitats across northeastern Thailand, yet its species diversity and chemical characteristics remain poorly understood. This study presents a novel integrated approach combining morphological identification, *rbc*L-based molecular analysis, and chemical profiling (LC-MS and FTIR) to comprehensively characterize Thai *Spirogyra* species. Six *Spirogyra* samples were collected from different water resources in Sakon Nakhon province and identified using both morphological characteristics and ribulose-bisphosphate carboxylase (*rbc*L) gene sequences. The sequence data of the *rbc*L gene was analyzed by using the database of the National Center for Biotechnology Information (NCBI). The results found that 6 *Spirogyra* samples were able to be identified as 3 *Spirogyra submaxima* and 1 sample each of *S. fluviatilis, S. maxima, and S. chungkingensis*. All *Spirogyra* samples were extracted with ethanol, yielding 6 crude ethanol extracts (SPE1 - SPE6). The chemical compositions were analyzed using Liquid Chromatography-Mass Spectrometry (LC-MS). LC-MS analysis of the 6 crude ethanol extracts revealed a total of 60 compounds, of which thirty were consistently detected across all *Spirogyra* samples, while the remaining compounds were specific to individual extracts. In addition, the FTIR profiles of SPE1-SPE6 were examined using the ATR-FTIR technique. The FTIR spectra indicated similar functional groups across samples, with absorption bands attributed to hydroxyl groups, CH_2 and CH_3 stretching vibrations, and carbonyl functionalities. These findings demonstrate that integrating morphological, genetic, and chemical analyses provides a more reliable framework for distinguishing *Spirogyra* species and reveals locality-specific chemical variation that may be valuable for future biochemical and taxonomic research.

Keywords: *Spirogyra*, *rbc*L markers, Phylogenetic, Chemical compound

Introduction

Spirogyra is a significant local aquatic resource in Sakon Nakhon Province, Thailand, commonly found and widely used in local cuisine. Scientifically, *Spirogyra* are green algae, belong to the Class Zygnematophyceae, and are characterized by unbranched filaments with spiral chloroplasts [1-3]. The number of chloroplasts varies from singular to multiple, depending on the age of the cell and species [4,5]. *Spirogyra* are widespread and occur in a variety of habitats; there are 537 species, 83 varieties, and 53 forma reported globally [6], with at least 22 species identified in Thailand [4,5].

The identification of *Spirogyra* is based on the morphological characteristics of vegetative cells and the aggregation patterns of reproductive cells, as well as the process of spore formation [7,8]. It is known that these morphological forms have been found to be variable, especially in laboratory conditions. Some In addition, molecular genetic techniques have been applied by analyzing nucleotide sequences of specific genes to assess genetic relationships. The ribulose-biphosphate carboxylase (*rbc*L) gene is frequently employed as a reliable genetic marker, which located in the chloroplast and responsible for carbon dioxide fixation during photosynthesis. These sequences were present in many green algae species, including *Spirogyra*, and the advantage of using the *rbc*L gene is the provision of high-quality nucleotide sequences, making it a preferred DNA marker for constructing DNA barcodes [9,10].

In the past, many research efforts have focused on the phytochemical composition of *Spirogyra*, which is derived from its general metabolic processes. As a result of these metabolic activities, algae like *Spirogyra* typically produce a variety of phytochemical agents, including fatty alcohols, terpenes, carotenoids, phytol, phenolic compounds, and neutral lipids such as fatty acids and esters [11-14]. These compounds contribute to the biological activities and nutritional contents of *Spirogyra*, highlighting its potential as a natural source for food products, supplements, and medicinal applications [11,15].

The study of *Spirogyra* in Sakon Nakhon province, Thailand, has previously found their distribution in several areas, exhibiting morphological differences in terms of size, shape, and the number of chloroplasts observed. There have also been studies on antibacterial properties, nutritional contents, total phenolic content, and phytochemical composition [11,16,17], but molecular biology research and other essential compounds have not yet been investigated concurrently. This study presents a novel, integrated approach combining morphological, molecular (*rbc*L), and chemical analyses to characterize *Spirogyra* species from multiple freshwater habitats in Sakon Nakhon. This information will contribute to enhancing the value of local resources and serve as a guideline for their future utilization.

Materials and methods

Determine the sampling sites

A survey of Sakon Nakhon province's water resources revealed the presence of *Spirogyra*. Then, determined the sampling points geographically (**Table 1**) and collected *Spirogyra* samples in the field for laboratory study.

Table 1 Sampling points.

Samples	Location	Geographic Coordinate	Area Characteristics
SP1	Ban Phon Ngam, Phon Ngam Subdistrict, Akat Amnuai District	17°41'21.8"N 103°57'38.4"E	Pond
SP2	Ban Nong Pling, Nong Pling Subdistrict, Nikhom Nam Un District	17°10'26.4"N 103°42'53.1"E	Pond
SP3	Ban Tao Ngoy, Tao Ngoy Subdistrict, Tao Ngoi District	16°59'09.5"N 104°10'05.6"E	Pond
SP4	Ban Tha Sa-ak, Khok Si Subdistrict, Sawang Daen Din District	17°37'14.2"N 103°24'07.4"E	Paddy field
SP5	Ban Khok Khon, Khok Si Subdistrict, Sawang Daen Din District	17°38'24.0"N 103°25'14.5"E	Pond
SP6	Khlong Phuong, Natal Subdistrict, Tao Ngoi District	16°59'45.8"N 104°10'25.1"E	River

Study of *Spirogyra* morphology

The collected *Spirogyra* samples assigned as SP1-SP6 according to the sampling site were cleaned, prepared as a wet mount slide, and observed under a light microscope (Nikon Eclipse E200). The morphology of algae was studied, including the width

and length of cells, number of chloroplasts, the number of chloroplasts turnover, and characteristics of the septum between cells using books and documents such as Takano *et al.* [8]; John *et al.* [18]; Stancheva *et al.* [19]. The samples were photographed by trinocular microscope (Euromex iScope series).

Study in molecular biology

Samples of *Spirogyra* collected from each sampling site were washed to remove as many contaminants as possible. Then, the samples were dried by blotting and placed into tea bags. The samples were stored in boxes containing desiccant packets (silica gel), and the boxes were sealed tightly [20]. *Spirogyra* can be diagnosed using molecular techniques by lysing the cells to extract DNA through grinding with glass beads. DNA was then extracted with Geneaid's Plant Genomic DNA Mini Kit (GP100) (Geneaid Biotech Ltd.) and verified on a 1% agarose gel. DNA fragments were amplified by the polymerase chain reaction (PCR) technique using a Taq DNA Polymerase master mix (Ampliqon brand). The primer targeted decoded genes in the chloroplast *rbc*L (ribulose-1,5-biphosphate carboxylase) sequence (forward primer RH1, 5'ATGTCACCACAAACAGAAACTAAAGC-3', and reverse primer 1385R, 5'AATTCAAATTTAATTTCTTTCC-3') [10]. PCR was performed with an initial 94 °C hold for 2 min, followed by 34 cycles of 94 °C for 30 s, 50 °C for 30 s, and 72 °C for 1 min 30 s, with a final extension at 72 °C for 4 min. PCR product was checked with 1% agarose gel against the GeneRuler 1 kb DNA Ladder (Thermo Scientific). Purify DNA fragments were purified by using DNA Clean & Concentrator (Zymo Research Corporation) and the base sequence analyzed using BioLign version 4.0.6.2 and compared with the base sequence data available in the database (GenBank) of the National Center for Biotechnology Information (NCBI). Phylogenetic analyses were conducted using MEGA version 11. The phylogenetic trees were reconstructed by the Maximum Likelihood (ML) and Neighbor-Joining (NJ) methods based on *rbc*L sequences, with 1,000 bootstrap replicates to assess the robustness of each node. The Tamura-Nei model was applied as the best-fit nucleotide substitution model.

Preparation of crude extracts

Spirogyra samples were collected from each sampling site and washed to remove contaminants such as dust, sand, and benthos. The samples were dried at 45 °C for 48 h or until completely dried by a hot air oven, ground, and stored in an aluminum foil bag. A *Spirogyra* sample of 100 g was extracted with ethanol (2×150 mL, 72 h each) using the maceration technique at room temperature. After maceration, the mixtures were filtered through Whatman No. 1 filter paper, and the filtrates concentrated using a rotary evaporator. The extraction yielding all *Spirogyra* crude ethanol extracts (assigned as SPE1-SPE6) were stored at 4 °C until required for further analysis. Each sample was extracted once; therefore, the results represent qualitative chemical profiles rather than replicated quantitative data.

LC-MS qualitative analysis of *Spirogyra*

Chromatographic analysis was performed in an Agilent Poroshell 120 EC-C18 column (4.6×150 mm^2, 2.7 μm) using an Agilent 1290 Infinity LC instrument (Agilent Technologies, CA, USA) in conjunction with an Agilent 6540 series QTOF-MS Mass Spectrometry equipped with an ESI source, a diode-array detector (Agilent Technologies, CA, USA), using both positive and negative ions electrospray ionization. The column temperature was maintained at 35 °C. The samples were dissolved in 1 mg/mL methanol, filtered with a syringe filter PTFE 0.2 µm, added to the LC-MS vial, and analyzed. The mobile phase consisted of A, 0.1% of formic acid in water, and B, 0.1% of formic acid in acetonitrile. Separation of chemical compositions was conducted under the following conditions: t = 0 min, 5% B; t = 1 min, 5% B; t = 10 min, 17% B; t = 13 min, 17% B; t = 20 min, 100% B; t = 25 min, 100% B. The gradient was allowed to re-equilibrate as follows: t = 27 - 33 min, 5% B. The flow rate was 200 µL/min, with an injection volume of 1 µL [21]. Chemical composition identification was done using Agilent mass Hunter workstation software (Qualitative Analysis, version B.08.00, Agilent) and Personal Compound Database and Library (PCDL). Moreover, the MS data, MS/MS fragmentation profiles, and molecular formulas proposed by the MassHunter were compared with previous literature and databases, such as ScienceDirect and Scifinder^n, with additional searches conducted via

Google Scholar, to interpret the chemical compositions of the *Spirogyra* crude extracts [14,22-24]. Chemical compositions with PCDL scores higher than 80 and a mass error of < ±5 ppm were further selected for *m*/*z* verification and MS analysis [25].

FT-IR functional groups analysis

The screening of functional groups of SPE1-SPE6 were identified using Attenuated Total Reflectance Fourier Transform Infrared Spectroscopy (ATR-FTIR) with a Bruker INVENIO spectrophotometer (Germany). The IR spectrums were recorded in the mid-infrared area in absorbance mode over a wavelength of 4,000 - 650 cm^{-1}.

Results and discussion

Identification of *Spirogyra*

Spirogyra specimens collected from 6 sampling sites were photographed as shown in **Figure 1**. The general shape is a cylindrical cell; the chloroplast is spiral and light green in color. The morphological characteristics in each sample were studied, as presented in **Table 2**.

Samples SP1, SP4, and SP5 show similar morphology; vegetative cell widths range from 67 - 83 µm and lengths from 81 - 136 µm, with 8 - 9 chloroplasts per cell and a single spiral turn. These studies were compared to the research of Stancheva *et al.* [19], who studied *Spirogyra* species in California streams and found that *Spirogyra submaxima* Transeau exhibits a cell width of 95 - 105 µm, cell length of 100 - 400 µm, and 8 - 9 chloroplasts per cell as well. Sherwood *et al.* [26] examined the diversity of green algae in the genus *Spirogyra* in the Hawaiian Islands. The study found that *Spirogyra submaximus* measures 78.7 - 121.5 µm, with an average of 7.4 chloroplasts per cell and 0.8 spirals. Notably, SP5 showed slightly shorter cells than SP1 and SP4, which may indicate intraspecific variability influenced by environmental factors [27].

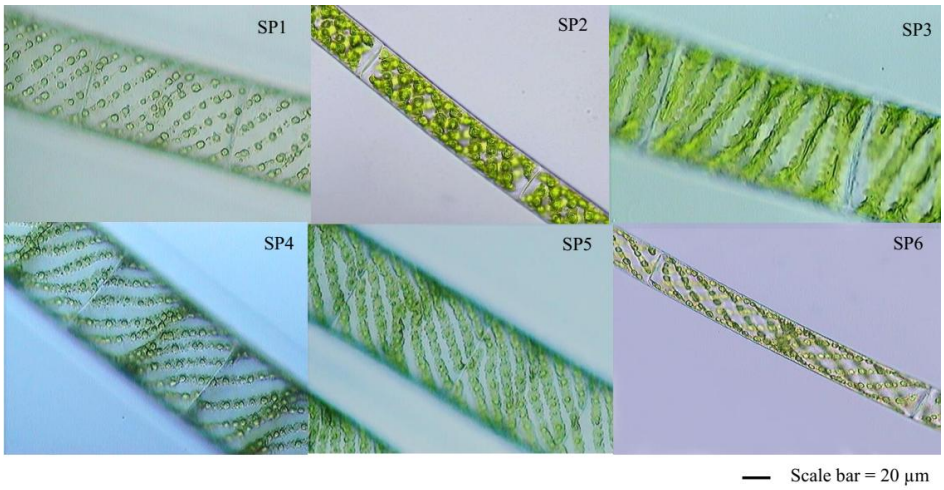

Figure 1 Micrograph of *Spirogyra* SP1-SP6.

Table 2 Morphological of 6 *Spirogyra* specimen.

Characteristics	SP1	SP2	SP3	SP4	SP5	SP6
Vegetative cell width (µm)	67 - 70	30 - 37	98 - 106	77 - 83	80 - 83	23 - 27
Vegetative cell length (µm)	97 - 110	125 - 140	169 - 260	113 - 136	81 - 117	193 - 206
End wall	Plane	Plane	Plane	Plane	Plane	Plane
Chloroplast per cell	8 - 9	3	4 - 5	8	8-9	3 - 4
Turns per cell	1	2 - 2.5	1 - 1.5	1	1	1 - 1.5
Species	*Spirogyra submaxima*	*Spirogyra fluviatilis*	*Spirogyra maxima*	*Spirogyra submaxima*	*Spirogyra submaxima*	*Spirogyra chungkingensis*

Note: Displayed as minimum-maximum values from 10 replicate samples.

SP2 demonstrated a narrow cell width (30 - 37 µm) and longer cell length (125 - 140 µm), with fewer chloroplasts (3 per cell) and 2 to 2.5 spiral turns per cell. These measurements correspond with the morphology reported for *Spirogyra fluviatilis* by John *et al*. [18] and El-Sheekh *et al*. [28], which showed vegetative cells 30 - 45 µm wide and 70 - 240 µm long, with 3 - 5 chloroplasts and 1.5 - 3.5 turns per cell. The size of the algae found in this study is smaller than that reported in the research by Stancheva *et al.* [19], which found cells with a maximum width of 45 µm and a maximum length of 240 µm. In the study by Phinyo *et al*. [29] this species of algae found in Chiang Rai province had a width of 50 - 58 µm and a length of 220 - 250 µm.

SP3 showed the largest cell dimensions, with widths of 98 - 106 µm and lengths ranging from 169 to 260 µm, containing 4 - 5 chloroplasts and 1 - 1.5 turns per cell. This morphology aligns well with *Spirogyra maxima*. This morphological feature closely resembles that of *Spirogyra maxima*. Research by Stancheva *et al.* [19]; Sherwood *et al*. [26]; John *et al.* [18] found that the cells were 118 - 150 µm wide and 90 - 280 µm long, with 5 - 8 chloroplasts per cell, each making 1.5 to 3 turns. And SP6 presented the narrowest cell width (23 - 27 µm) and the longest cell length (193 - 206 µm), with 3 - 4 chloroplasts and 1 to 1.5 spiral turns. These features are consistent with *Spirogyra chungkingensis* and similar to the research results of Takano *et al*. [8], which collected *Spirogyra* from pond or paddy fields in Japan and found *Spirogyra chungkingensis* had 24 - 27 µm width, 150 - 300 µm length, 3 chloroplasts, and 5 turns per cell.

These morphological observations support previous classifications, confirming the morphological diversity within the genus *Spirogyra* by using cell size, chloroplast number, and chloroplast turns as taxonomic markers. These characteristics result from responses to the environment, which are related to the physical and chemical factors of the water source [30], and are similar to Hainz *et al.* [31] research, which found that nutrients are an important factor that causes the formation of morphotype or filament-type groups. In environments with high nutrient levels, the width of the filament increases. Other factors, such as ions, buffering capacity, light intensity, and water temperature, do not have a significant effect on the formation of different shapes. Contrary to the research findings of Berry and Lembi [7], they found that morphological characteristics vary as a result of responses to light and temperature. Under conditions of high light and temperature, which increase net photosynthesis, *Spirogyra* was observed to grow longer, exceeding 100 µm. Because environmental factors affect morphology variation, species identification based on morphology may be confused. Additionally, specimens correctly identified at the time of collection may later exhibit characteristics similar to other species [10]. The features of the reproductive process are also important for species identification, including the type of conjugation and characteristics of the mature zygospore wall, such as zygospore ornamentation, shape, and color [3,19,31]. However, vegetative filaments of *Spirogyra* can occur throughout the year, but reproductive filaments are rather rare in the field [19]; only 10% of *Spirogyra* in natural water resources are found in the sexual reproductive stage [31]. On the other hand, stress conditions such as temperature, drought, and pH induce the formation of conjugation tubes of *Spirogyra* genera [27,28], but difficulty in inducing conjugation in the laboratory and the mutation rate can occur once per generation [10]. Therefore, many studies have used filaments collected from native habitats [28], alongside molecular techniques which are effective for both accurately identifying and analyzing genetic variation.

In molecular identification of *Spirogyra*, the chloroplast *rbc*L gene is widely recognized as a reliable and universal genetic marker, providing high-quality nucleotide sequences suitable for species-level classification. In this study, the *rbc*L gene was successfully amplified using specific primers, and the resulting DNA fragments were analyzed by PCR. The obtained nucleotide sequences were compared with the NCBI GenBank database, and species identification was further confirmed by constructing phylogenetic trees using the Maximum Likelihood (ML) and Neighbor-Joining (NJ) methods, in conjunction with morphological observations.

The BLAST sequence alignment revealed that isolates SP1, SP4, and SP5 shared high identity percentages with *Spirogyra submaxima* strain RSS021 (99.23%, 98.64%, and 99.38%, respectively). Isolate SP2 showed the highest similarity to *S. fluviatilis*, while

SP3 was closely related to *S. maxima* (98.46%) and SP6 to *S. chungkingensis* (99.84%). These results indicate a high degree of genetic relatedness between the studied isolates and previously characterized *Spirogyra* species.

The phylogenetic relationships among the isolates were further analyzed based on the *rbc*L sequences (**Figures 2** and **3**). Both the ML and NJ analyses consistently separated the isolates into 4 distinct clades corresponding to reference *Spirogyra* species, reflecting considerable genetic diversity among the samples. In the ML tree, Clade I contained isolate SP2, which clustered with *S. fluviatilis* but exhibited low bootstrap support (51%), indicating weak confidence in this relationship. Clade II included isolate SP6 grouped with *S. chungkingensis* (65%), while Clade III comprised isolate SP3 associated with *S. maxima* (approximately 60% - 70%). These moderate bootstrap values suggest partial but not conclusive support for species-level assignment. In contrast, Clade IV, composed of isolates SP1, SP4, and SP5, displayed high bootstrap support (98%), confirming a strong genetic affinity with *S. submaxima.*

The NJ phylogenetic tree showed a topology consistent with the ML tree but with slightly higher bootstrap values (98% - 99%), indicating stable clustering patterns across analytical methods. The consistency between the ML and NJ topologies reinforces the robustness of the inferred evolutionary relationships, while the variation in bootstrap values highlights methodological influences and potential limitations of single-gene analyses.

High bootstrap support, such as that observed for Clade IV, is generally considered strong evidence for reliable evolutionary relationships and provides confidence in the identification of isolates SP1, SP4, and SP5 as *S. submaxima.* Conversely, the weak support in Clade I suggests uncertainty in the placement of SP2 with *S. fluviatilis*, possibly due to limited sequence divergence, intra-species variability, or insufficient phylogenetic signal within the *rbc*L gene. Similar findings have been reported in previous studies, where *rbc*L-based phylogenies provided valuable taxonomic information but limited resolution among closely related or morphologically similar *Spirogyra* taxa [19].

The differences in bootstrap values between the ML and NJ methods further demonstrate the influence of model assumptions and computational algorithms on phylogenetic inference. Given that *rbc*L is a relatively conserved chloroplast gene, it may not capture sufficient nucleotide variability to resolve recent divergence events within *Spirogyra*. To enhance the phylogenetic resolution, future studies should combine *rbc*L with additional molecular markers, such as nuclear 18S rDNA or ITS-2 regions, providing a more comprehensive framework for taxonomic clarification.

Overall, the results confirm that *rbc*L is a suitable and reliable marker for preliminary molecular identification and for delineating major *Spirogyra* lineages. The strong bootstrap-supported clades validate its use in genus-level and some species-level identification. However, weakly supported nodes emphasize the need for a multi-locus approach to achieve a clearer understanding of the evolutionary relationships and species boundaries within *Spirogyra*.

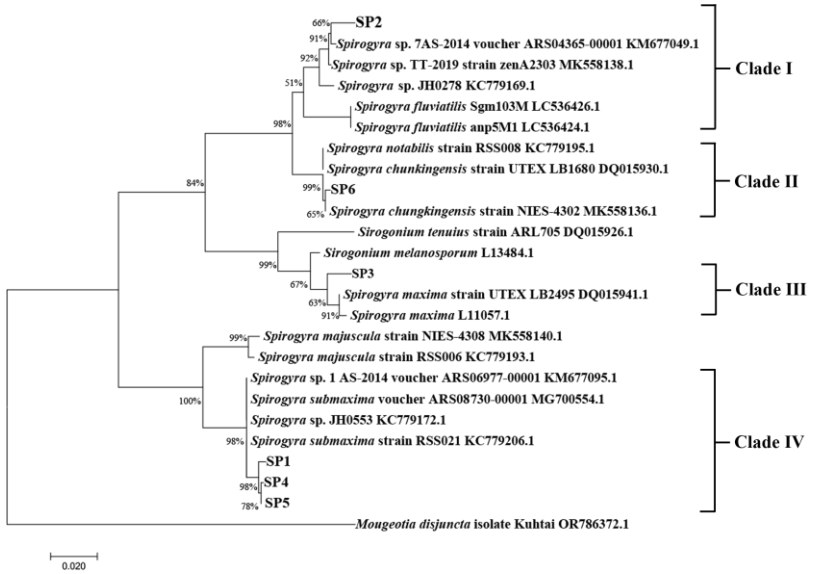

Figure 2 Phylogenetic tree by Maximum Likelihood method at 1,000 bootstraps (100%) of *Spirogyra* samples in *rbc*L gene locus (Only values > 50% shown).

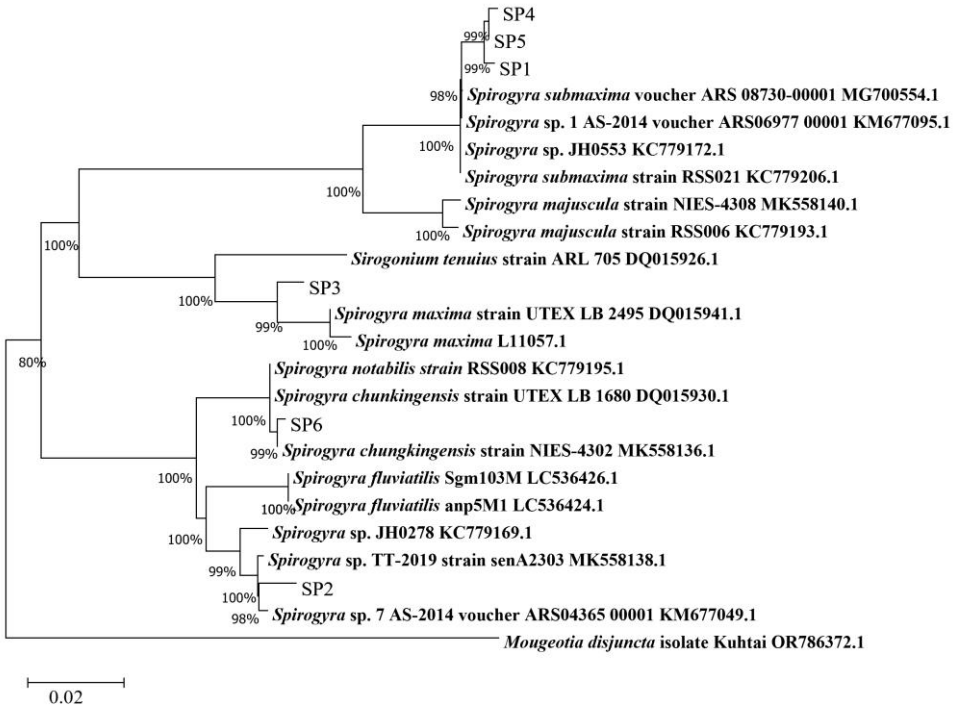

Figure 3 Phylogenetic tree by neighbor-joining method at bootstrap 1,000 times (100%) of *Spirogyra* samples in *rbc*L gene locus (Only values > 50% shown).

Qualitative profiling of *Spirogyra* samples SP1-SP6 using LC-MS method

Six *Spirogyra* samples were successfully extracted with ethanol yielding crude ethanol extracts SPE1-SPE6. Six *Spirogyra* samples were initially screened and their chemical compositions determined using LC-MS. The base peak chromatograms of SPE1-SPE6 were obtained as shown in **Figure 4**. The data for the identified compounds in positive and negative mode, such as the retention time (RT), the chemical formular, the molecular mass, the mass-to-charge ratio (*m*/*z*), and the mass error < ±5 ppm, are summarized in **Tables 3** and **4**. All the compounds in the 6 *Spirogyra* crude extracts were identified using the Personal Compound Database and Library (PCDL). The experimental molecular formula correctly matched the quasi-

molecular ions, theoretical molecular ions, and fragment ions, as shown by the mass error for molecular ions in all detected compounds being within < ±5 ppm.

The qualitative identification of the chemical composition of all *Spirogyra* crude ethanol extracts found 54 and 45 compounds in positive and negative modes, respectively. Among the 6 *Spirogyra* extracts (SPE1-SPE6), nine compounds in positive ionization mode (**Figure 5**) and 21 compounds in negative ionization mode (**Figure 6**) were consistently detected across all samples. These consistently present compounds may represent potential biomarkers of *Spirogyra* species, reflecting shared chemical traits. However, further quantitative and functional studies are required to confirm their biomarker status. The compounds that were commonly identified in all 6 samples serve as potential chemical markers, indicating their specificity to *Spirogyra* found in Sakon Nakhon, Thailand. Distinct metabolites were detected across SPE1-SPE6. Hexanedioic acid bis(2-ethylhexyl) ester and 1-octadecanol were exclusively detected in SPE1. In SPE2, 1-octadecanol, 4-ethenyl-2-methoxyphenol, 8-hexadecyne, 2,4,4-trimethyl-3-(3-oxo-1-butenyl)-2-cyclohexen-1-one, 9,12-octadecadienoic acid methyl ester, and (*Z*,*Z*)-9,12-octadecadienoic acid ethyl ester were identified, whereas oleic acid and propanoic acid anhydride were exclusively detected in SP3. SP5 contained 4-hydroxy-4-methyl-2-pentanone, hexadecane, and 4,8,12,16-tetramethylheptadecan-4-olide, while (3*β*)-stigmasta-5,24(28)-dien-3-ol and cyclotetracosane were uniquely found in SPE6. Notably, SPE4 exhibited the highest diversity, with eight exclusive metabolites: 4-methyl-2-heptanone, decane, (*Z*)-3-heptadecen-5-yne, 4-ethenyl-2-methoxyphenol, (*Z*)-octa-9-decenamide, (2*E*,7*R*,11*R*)-3,7,11,15-tetramethyl-2-hexadecen-1-ol, 4,8,12,16-tetramethylheptadecan-4-olide, and hexanedioic acid bis(2-ethylhexyl) ester. The findings suggest that *Spirogyra* collected from different locations exhibit broadly similar overall chemical compositions, yet notable variations exist in specific constituent compounds.

In addition, loliolide and hexadecanoic acid methyl ester were not only found in SPE1-SPE6 but also in *Spirogyra porticalis* [23]. 6,10,14-Trimethyl-2-pentadecanone and linoleic acid were found from *Spirogyra neglecta* [11,32]. *Spirogyra rhizoides* and SPE1-SPE6 linolenic acid, linoleic acid, and 9-cctadecenoic acid were observed [33]. Variations in specific constituent compounds are strongly influenced by environmental and nutritional factors, such as light intensity and duration, CO_2 concentration, pH, temperature, nutrient availability, and biotic interactions [34]. Nutrient input emerged as the dominant factor, influencing the production of all 6 chemical classes (phenolics, pigments, polysaccharides, sterols, diterpenes, and fatty acids). In contrast, hydrodynamics and salinity had a smaller overall impact, primarily affecting pigments (hydrodynamics) and phenolic compounds (hydrodynamics and salinity) [35]. Furthermore, allelopathic effects from SPE1-SPE6 involve the release of distinct secondary metabolites into the environment, thereby influencing the growth, survival, and reproduction of other organisms [36].

Variation in chemical composition is responsible for many biological activities. *Spirogyra* green algae showed notable in vivo anti-leishmanial efficacy in BALB/c mice [37]. The anti-inflammatory activity of *Spirogyra neglecta* is mediated through the inhibition of nitric oxide (NO) production [11]. Ethanol crude extracts of 6 *Spirogyra* spp. exhibited antimicrobial activity against *Candida* sp., *Staphylococcus aureus*, and *Escherichia coli* [17]. Eleven green algae species from Sindh (Pakistan) exhibited significant phytotoxic activity but showed non-significant cytotoxic, insecticidal, and antitumor activities [38]. Moreover, *Spirogyra aequinoctialis*, *Spirogyra pratensis* and *Spirogyra subsalsa* exhibited significant phytotoxic activity against *Lemna minor* [39].

The LC-MS analysis in this study provides a qualitative overview of metabolite diversity among *Spirogyra* samples. Many identified compounds are common fatty acids and esters; therefore, the focus is on comparing shared versus sample-specific metabolites rather than assigning unique biomarkers. Variation among samples may reflect ecological differences, but detailed correlations will require further quantitative and environmental investigations.

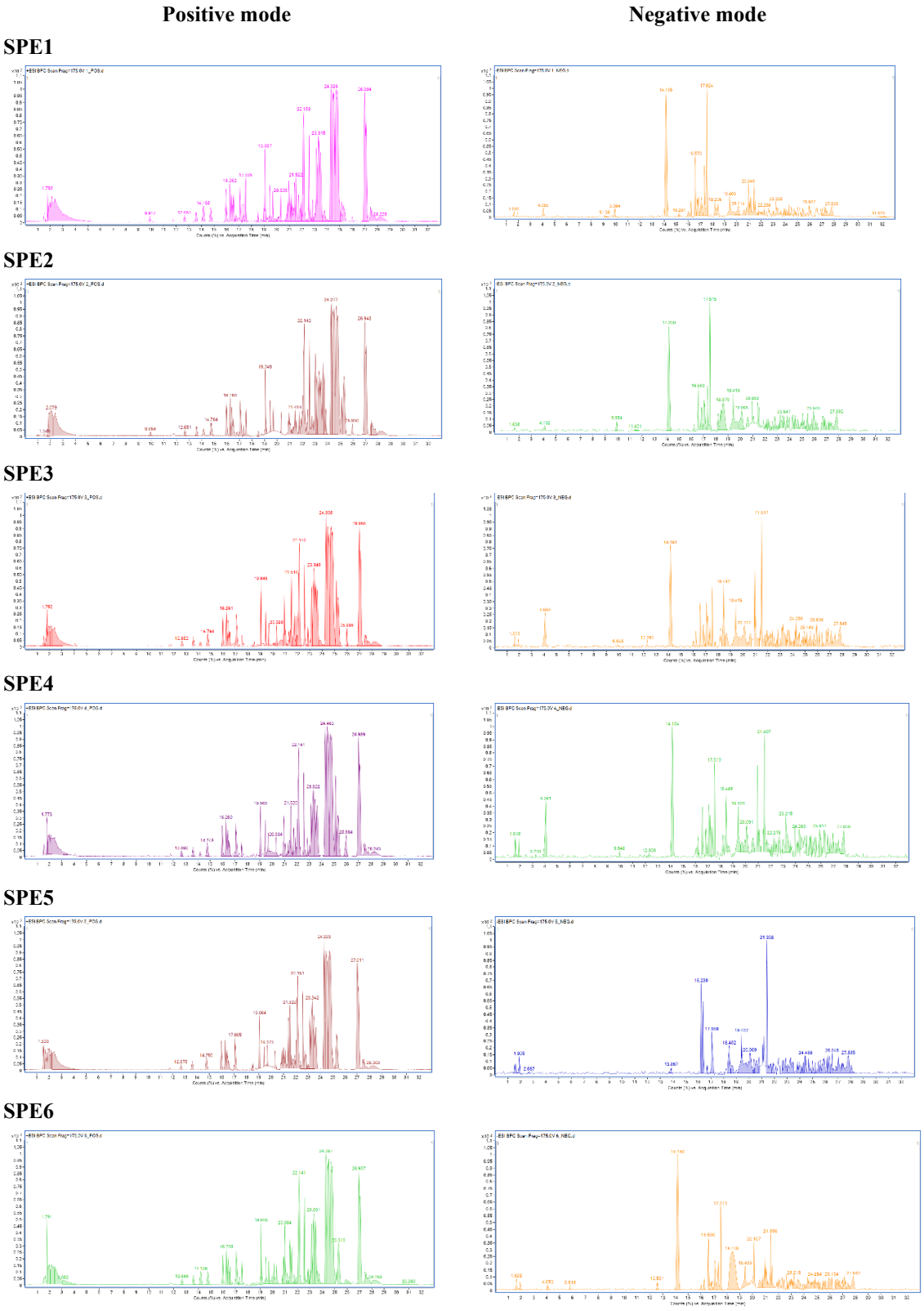

Figure 4 Positive and negative modes chromatograms of SPE1-SPE6 by LC-MS.

Table 3 Identified compounds from SPE1-SPE6 by LC-MS (positive mode).

No	RT (min)[1]	Mass	*m/z* (Expected)[2]	Chemical Formular	Error (ppm)[3]	Identification	Samples (SPE)					
							1	2	3	4	5	6
1	15.312	196.1096	197.1169	$C_{11}H_{16}O_3$	−1.79	Loliolide	✓	✓	✓	✓	✓	✓
2	16.477	374.1520	392.1874	$C_{24}H_{22}O_4$	0.60	Phthalic acid, di(3,4-dimethylphenyl) ester	✓	✓				✓
3	17.094	206.1517	229.1411	$C_{10}H_{22}O_4$	−0.71	Oleic acid			✓			
4	17.357	116.0832	139.0724	$C_6H_{12}O_2$	−4.59	4-hydroxy-4-methyl-2-Pentanone				✓	✓	
5	17.525	130.0636	153.0528	$C_6H_{10}O_3$	4.40	Propanoic acid anhydride			✓			
6	17.714	128.1210	151.1094	$C_8H_{16}O_6$	0.27	4-methyl-2-Heptanone				✓		
7	19.057	256.2398	274.2736	$C_{16}H_{32}O_2$	−1.82	Tetradecanoic acid, 12-methyl-, methyl ester	✓	✓		✓		✓
8	19.091	212.2133	230.2472	$C_{14}H_{28}O$	−3.14	Tetradecanal		✓		✓		✓
9	19.366	182.2042	200.2368	$C_{13}H_{26}$	4.24	2,5-dimethyl-2-Undecene	✓					
10	19.408	208.1467	209.1540	$C_{13}H_{20}O_2$	1.97	4-(2,2,6-trimethyl-7-oxabicyclo [4.1.0] hept-1-yl)-3-Buten-2-one	✓	✓	✓	✓	✓	✓
11	19.435	180.1153	181.1226	$C_{11}H_{16}O_2$	1.42	Dihydroactinidiolide	✓	✓	✓	✓		✓
12	19.475	270.2546	288.2884	$C_{17}H_{34}O_2$	−4.82	Hexadecanoic acid, methyl ester		✓				✓
13	19.553	286.2498	304.2835	$C_{17}H_{34}O_3$	−3.50	Hexadecanoic acid, 2-hydroxy-, methyl ester		✓			✓	✓
14	19.598	142.1728	165.1620	$C_{10}H_{22}$	4.48	Decane				✓		
15	19.623	210.2347	228.2680	$C_{15}H_{30}$	−0.40	1-Pentadecene		✓	✓	✓		✓
16	19.758	270.2932	293.2826	$C_{18}H_{38}O$	3.48	1-Octadecanol		✓				
17	19.533	196.2186	214.2524	$C_{14}H_{28}$	−2.74	Tetradecene	✓	✓			✓	✓
18	20.118	232.1827	233.1900	$C_{16}H_{24}O$	−0.07	1-Hexadecanol	✓					✓
19	20.320	298.2865	316.3204	$C_{19}H_{38}O_2$	−2.33	Octadecanoic acid, methyl ester			✓	✓	✓	✓
20	20.416	184.2197	207.2090	$C_{13}H_{28}$	3.18	Tridecane						✓
21	20.626	228.2099	251.1991	$C_{14}H_{28}O_2$	4.11	Tetradecanoic acid (Myristic acid)		✓			✓	
22	20.650	242.2241	265.2134	$C_{15}H_{30}O_2$	−1.78	Pentadecanoic acid (Pentadecylic acid)	✓		✓	✓	✓	✓
23	20.892	226.2661	249.2556	$C_{16}H_{31}$	0.43	Hexadecane					✓	

No	RT (min)[1]	Mass	*m/z* (Expected)[2]	Chemical Formular	Error (ppm)[3]	Identification	Samples (SPE)					
							1	2	3	4	5	6
24	20.904	220.1826	221.1896	$C_{15}H_{24}O$	−0.34	2,6-bis(1,1-dimethylethyl)-4-methylPhenol	✓	✓	✓	✓		✓
25	21.023	150.0677	151.0750	$C_9H_{10}O_2$	−2.80	4-ethenyl-2-methoxyPhenol		✓				
26	21.140	266.2970	284.3308	$C_{19}H_{38}$	−1.49	1-Nonadecene	✓	✓	✓	✓	✓	✓
27	21.267	324.3027	342.3369	$C_{21}H_{40}O_2$	−0.45	4,8,12,16-Tetramethyl-heptadecan-4-olide					✓	
28	21.374	222.2353	245.2246	$C_{16}H_{30}$	2.54	8-Hexadecyne		✓				
29	21.408	330.2783	331.2857	$C_{19}H_{38}O_4$	3.81	Hexadecanoic acid, 2-hydroxy-1-(hydroxymethyl) ethyl ester	✓	✓	✓	✓	✓	✓
30	21.497	278.2251	279.2323	$C_{18}H_{30}O_2$	1.82	*α*-Linolenic acid	✓		✓		✓	
31	21.549	206.1304	207.1376	$C_{13}H_{18}O_2$	−1.29	2,4,4-trimethyl-3-(3-oxo-1-butenyl)-2-Cyclohexen-1-one		✓				
32	21.575	212.2501	235.2393	$C_{15}H_{32}$	−1.43	Pentadecane		✓		✓	✓	✓
33	21.701	280.2411	281.2467	$C_{18}H_{32}O_2$	2.95	Linoleic acid	✓		✓	✓	✓	✓
34	21.749	264.2084	265.2153	$C_{17}H_{28}O_2$	−1.92	7,10,13-Hexadecatrienoic acid, methyl ester	✓	✓	✓		✓	✓
35	22.014	312.3030	313.3106	$C_{20}H_{40}O_2$	0.51	Arachidic acid			✓			✓
36	22.240	234.2343	235.2419	$C_{17}H_{30}$	−1.77	(*Z*)-3-Heptadecen-5-yne				✓		
37	22.527	266.1678	267.1750	$C_{19}H_{22}O$	2.62	1,3-diphenyl-4,4-dimethyl-1-Penten-3-ol	✓	✓	✓	✓	✓	✓
38	22.617	268.2398	291.2303	$C_{17}H_{32}O_2$	−1.67	(*Z*)-9-Hexadecenoic acid, methyl ester	✓	✓	✓		✓	✓
39	22.711	390.2779	413.2670	$C_{24}H_{38}O_4$	2.31	(*Z*)-9-Hexadecenoic acid, methyl ester		✓	✓	✓	✓	✓
40	23.063	284.2719	285.2791	$C_{18}H_{36}O_2$	1.41	Heptadecanoic acid, methyl ester	✓	✓	✓	✓	✓	✓
41	23.052	292.2402	315.2292	$C_{19}H_{32}O_2$	0.06	9,12,15-Octadecatrienoic acid, methyl ester		✓	✓	✓	✓	✓
42	23.150	138.1047	156.1385	$C_9H_{14}O$	1.79	3,5,5-Trimethyl-2-cyclohexene-1-one (Isophorone)	✓	✓	✓	✓	✓	✓
43	23.150	155.1313	156.1385	$C_9H_{17}NO$	2.04	2,2,6,6-tetramethyl-4-Piperidinone	✓	✓	✓	✓	✓	✓

No	RT (min)[1]	Mass	*m*/*z* (Expected)[2]	Chemical Formular	Error (ppm)[3]	Identification	Samples (SPE)					
							1	2	3	4	5	6
44	24.115	308.2723	309.2793	$C_{20}H_{36}O_2$	2.46	9,12-Octadecadienoic acid (*Z*,*Z*)-, ethyl ester		✓	✓	✓	✓	✓
45	24.634	278.2258	279.2330	$C_{18}H_{30}O_2$	4.41	*α*-Linolenic acid		✓		✓		✓
46	24.634	396.3756	397.3829	$C_{29}H_{48}$	0.12	Stigmastan-3,5-diene		✓	✓		✓	✓
47	24.716	264.2455	282.2793	$C_{18}H_{32}O$	0.79	(*Z*,*Z*,*Z*)-9,12,15-Octadecatrien-1-ol,	✓	✓	✓	✓		✓
48	24.716	281.2720	282.2793	$C_{18}H_{35}NO$	0.62	(*Z*) -9-Octadecenamide	✓	✓	✓	✓	✓	✓
49	24.887	336.3030	354.3369	$C_{22}H_{40}O2$	0.61	Docosadienoic acid					✓	✓
50	25.154	370.3085	393.2981	$C_{22}H_{42}O_4$	0.63	Hexanedioic acid, bis(2-ethylhexyl) ester	✓					
51	25.240	412.3697	413.3774	$C_{29}H_{48}O$	−2.09	(3*β*)-Stigmasta-5,24(28)-dien-3-ol						✓

Note: [1]RT = Retention time; [2]*m*/*z* = Mass-to-charge ratio; [3]Mass error (ppm) = The difference between the experimentally measured mass of a molecule and its theoretical exact mass < ±5 ppm.

Table 4 Identified compounds from SPE1-SPE6 by LC-MS (negative mode).

No	RT (min)[1]	Mass	*m*/*z* (Expected)[2]	Chemical Formular	Error (ppm)[3]	Identification	Samples (SPE)					
							1	2	3	4	5	6
1	1.783	130.0626	175.061	$C_6H_{10}O_3$	−3.17	Propanoic acid, anhydride	✓	✓	✓	✓	✓	✓
2	9.243	93.0578	138.0561	C_6H_7N	−0.24	2-Methylpyridine			✓	✓	✓	
3	9.243	139.0632	138.0561	$C_7H_9NO_2$	−1.11	3-ethyl-4-1H-Pyrrole-2,5-dione			✓	✓	✓	
4	10.611	116.0832	115.0762	$C_6H_{12}O_2$	−4.20	4-hydroxy-4-methyl-2-Pentanone	✓	✓	✓	✓	✓	✓
5	17.469	98.0731	157.0870	$C_6H_{10}O$	−0.41	4-methyl-3-Penten-2-one	✓	✓	✓	✓	✓	✓
6	17.839	196.1092	241.1079	$C_{11}H_{16}O_3$	−3.54	Loliolide		✓		✓	✓	✓
7	17.847	138.1046	183.1029	$C_9H_{14}O$	1.06	3,5,5-trimethyl-2-Cyclohexene-1-one (Isophorone)	✓	✓	✓	✓	✓	✓
8	18.252	128.1204	173.1186	$C_8H_{16}O$	1.87	4-methyl-2-Heptanone	✓	✓	✓	✓	✓	✓
9	18.730	150.0682	209.0818	$C_9H_{10}O_2$	1.02	4-ethenyl-2-methoxyPhenol				✓		
10	19.383	180.1150	179.1079	$C_{11}H_{16}O_2$	−0.36	Dihydroactinidiolide	✓	✓	✓	✓	✓	✓
11	20.066	208.1463	207.1392	$C_{13}H_{20}O_2$	−0.16	4-(2,2,6-trimethyl-7-oxabicyclo [4.1.0]	✓	✓	✓	✓	✓	✓

No	RT (min)[1]	Mass	*m/z* (Expected)[2]	Chemical Formular	Error (ppm)[3]	Identification	Samples (SPE)					
							1	2	3	4	5	6
						hept-1-yl)-3-Buten-2-one						
12	20.190	220.1828	265.1810	$C_{15}H_{24}O$	0.46	2,6-bis(1,1-dimethylethyl)-4-methyl Phenol	✓	✓	✓	✓		✓
13	20.215	264.2091	309.2074	$C_{17}H_{28}O_2$	0.72	7,10,13-Hexadecatrienoic acid, methyl ester	✓	✓	✓	✓	✓	✓
14	20.357	268.2403	313.2386	$C_{17}H_{32}O_2$	0.35	(*Z*)-9-Hexadecenoic acid, methyl ester	✓	✓	✓	✓	✓	✓
15	20.425	228.2079	287.2226	$C_{14}H_{28}O_2$	−4.59	Tetradecanoic acid (Myristic acid)	✓	✓		✓	✓	✓
16	20.589	280.1867	339.2006	$C_{17}H_{28}OS$	2.16	1,5-Hexadien-3-ol, 3-methyl-6-(methylthio)-1-(2,6,6-trimethyl-1-cyclohexen-1-yl)	✓	✓	✓	✓	✓	✓
17	20.813	270.2558	315.2543	$C_{17}H_{34}O_2$	−0.24	Hexadecanoic acid, methyl ester	✓	✓	✓	✓	✓	✓
18	21.094	292.2393	351.2534	$C_{19}H_{32}O_2$	−3.14	9,12,15-Octadecatrienoic acid, methyl ester			✓	✓		
19	21.266	232.1828	291.1968	$C_{16}H_{24}O$	0.57	1-Hexadecanol	✓	✓	✓	✓	✓	✓
20	21.489	242.2237	287.2230	$C_{15}H_{30}O_2$	−3.55	Pentadecanoic acid (Pentadecylic acid)	✓	✓	✓	✓	✓	
21	21.815	270.2930	269.2856	$C_{18}H_{38}O$	2.65	1-Octadecanol	✓					
22	21.903	294.2550	353.2688	$C_{19}H_{34}O_2$	−2.86	9,12-Octadecadienoic acid, methyl ester		✓				
23	21.903	308.709	353.26902	$C_{20}H_{36}O_2$	−2.07	(*Z*, *Z*)-9,12-Octadecadienoic acid ethyl ester		✓				
24	22.132	256.2398	315.2541	$C_{16}H_{32}O_2$	−1.54	12-methyl-Tetradecanoic acid, methyl ester	✓	✓	✓		✓	✓
25	22.132	212.2142	211.2066	$C_{14}H_{28}O$	0.66	Tetradecanal	✓	✓	✓	✓	✓	✓
26	22.616	182.2037	227.2016	$C_{13}H_{26}$	1.36	2,5-dimethyl-2-Undecene	✓	✓	✓	✓	✓	✓
27	22.822	286.2509	285.2436	$C_{17}H_{34}O_3$	0.25	2-hydroxy-Hexadecanoic acid, methyl ester	✓	✓	✓	✓	✓	✓
28	22.831	336.3747	395.3887	$C_{24}H_{48}$	−2.54	Cyclotetracosane						✓

No	RT (min)[1]	Mass	*m*/*z* (Expected)[2]	Chemical Formular	Error (ppm)[3]	Identification	Samples (SPE)					
							1	2	3	4	5	6
29	23.093	330.2771	329.2699	$C_{19}H_{38}O_4$	0.40	Hexadecanoic acid, 2-hydroxy-1-(hydroxymethyl) ethyl ester			✓		✓	✓
30	23.228	278.2248	277.2176	$C_{18}H_{30}O_2$	0.93	*α*-Linolenic acid	✓	✓	✓	✓	✓	✓
31	23.854	281.2717	326.2699	$C_{18}H_{35}NO$	−0.63	(*Z*)-Octa-9-decenamide				✓		
32	23.989	296.3077	355.3217	$C_{20}H_{40}O$	−0.70	(2*E*,7*R*,11*R*)-3,7,11,15-tetramethyl-2-Hexadecen-1-ol	✓			✓		
33	24.287	280.2406	279.2333	$C_{18}H_{32}O_2$	1.25	Linoleic acid	✓	✓	✓	✓	✓	✓
34	24.287	234.2352	279.2334	$C_{17}H_{30}$	1.88	(*Z*)-3-Heptadecen-5-yne	✓	✓		✓	✓	✓
35	24.393	324.3026	369.301	$C_{21}H_{40}O_2$	−0.64	4,8,12,16-tetramethyl-Heptadecan-4-olide				✓		
36	24.393	370.3081	415.3069	$C_{22}H_{42}O_4$	−0.60	Hexanedioic acid, bis(2-ethylhexyl) ester				✓		
37	24.753	264.2445	323.2584	$C_{18}H_{32}O$	−3.08	(*Z*,*Z*,*Z*)-9,12,15-Octadecatrien-1-ol	✓	✓	✓	✓		
38	24.827	336.3024	395.3161	$C_{22}H_{40}O_2$	−1.32	Docosadienoic acid		✓		✓	✓	✓
39	24.83	284.2717	343.2856	$C_{18}H_{36}O_2$	0.75	Heptadecanoic acid, methyl ester	✓	✓	✓	✓		✓
40	24.83	298.2874	343.2856	$C_{19}H_{38}O_2$	0.74	Octadecanoic acid, methyl ester	✓	✓	✓	✓	✓	✓
41	25.832	268.2767	327.2906	$C_{18}H_{36}O$	0.27	6,10,14-trimethyl-2-Pentadecanone	✓	✓	✓	✓	✓	✓
42	25.982	210.2343	255.2324	$C_{15}H_{30}$	−2.37	1-Pentadecene	✓	✓	✓	✓	✓	✓
43	25.982	196.2186	255.2324	$C_{14}H_{28}$	−2.54	Tetradecene	✓	✓	✓	✓	✓	✓
44	26.139	222.2351	281.2490	$C_{16}H_{30}$	1.64	8-Hexadecyne	✓	✓	✓	✓	✓	✓
45	26.139	282.2563	281.2490	$C_{18}H_{34}O_2$	1.34	(*E*)-9-Octadecenoic acid	✓	✓	✓	✓	✓	✓

Note: [1]RT = Retention time; [2]*m*/*z* = Mass-to-charge ratio; [3]Mass error (ppm) = The difference between the experimentally measured mass of a molecule and its theoretical exact mass < ±5 ppm.

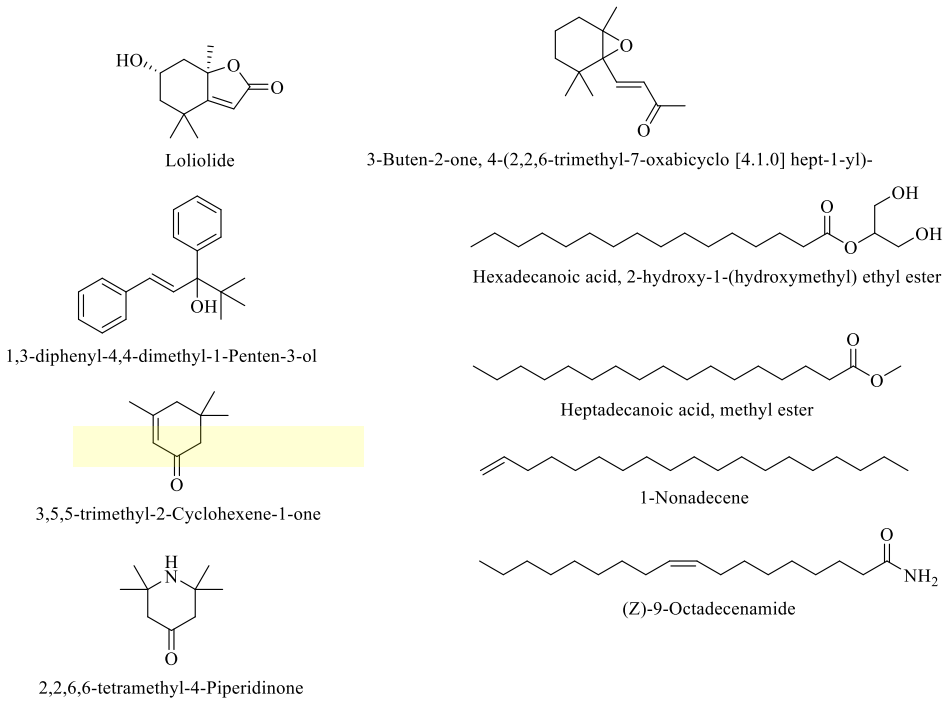

Figure 5 The similar chemical composition of SPE1-SPE6 (positive mode).

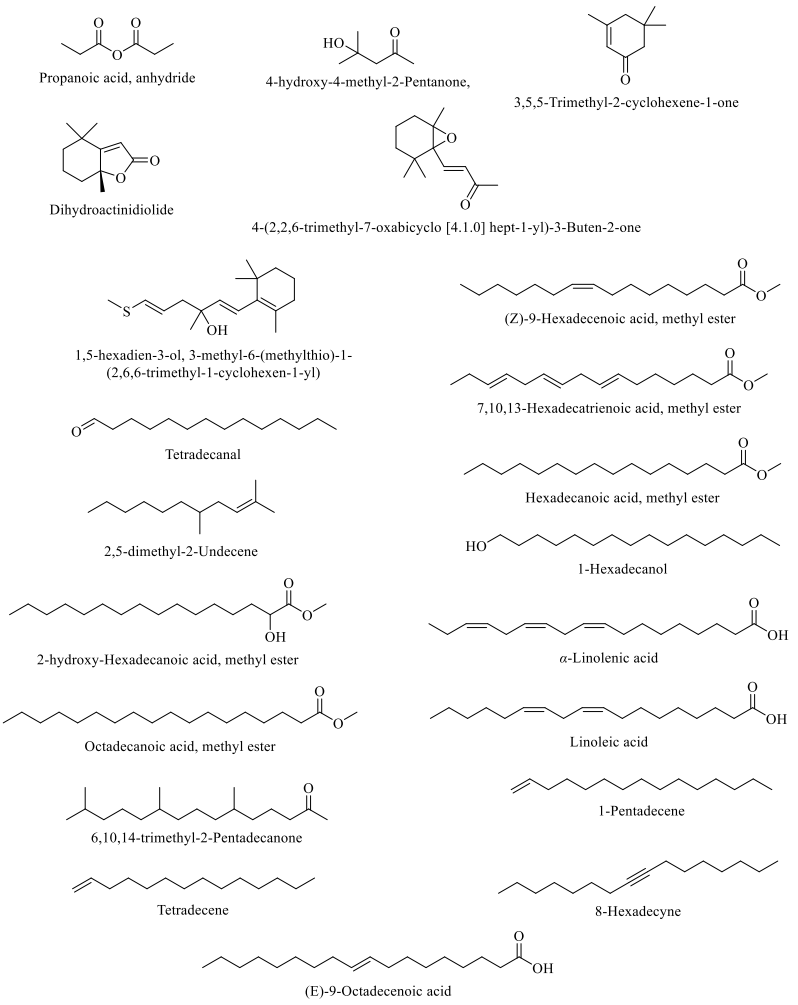

Figure 6 The similar chemical composition of SPE1-SPE6 (negative mode).

Functional group analysis using FT-IR technique

FTIR analysis was performed qualitatively to confirm major functional groups and to compare overall spectral patterns among samples, providing supportive information consistent with LC-MS results. FTIR spectra profile of SPE1-SPE6 exhibited high similarity across all peaks, as shown in **Figure 7**. The broad absorption band around 3,500 - 3,200 cm^{-1} is related to the presence of stretching vibrations of hydrogen bonds (hydroxyl groups -OH from carboxyls, phenols or alcohols). The peak at 2,800 - 3,000 cm^{-1} corresponds to the methylene -CH_2 and methyl -CH_3 groups of long linear alkane components (the asymmetric and symmetric stretching in aliphatic components). The peak at 1,700 cm^{-1} corresponds to the vibration of the C=O bond in the carbonyl group. In the FTIR spectra of SPE1-SPE6, several small and sharp peaks were detected between 1,600 and 1,000 cm^{-1}, corresponding to aromatic ring stretching (1,560 cm^{-1}), ionic carboxylate groups -COO^- (1420 cm^{-1}), C-O stretching (1,260 - 1,050 cm^{-1}), and C-O-C vibrations [40]. This evidence is consistent with the chemical compositions observed in all 6 *Spirogyra* species. SEP1-SEP6 displayed similar infrared (IR) spectra, likely reflecting the presence of common functional groups in the crude extracts. However, FTIR spectroscopy analysis shows only the functional groups in the crude extract and is insufficient to show the presence of different classes of chemical compositions [41].

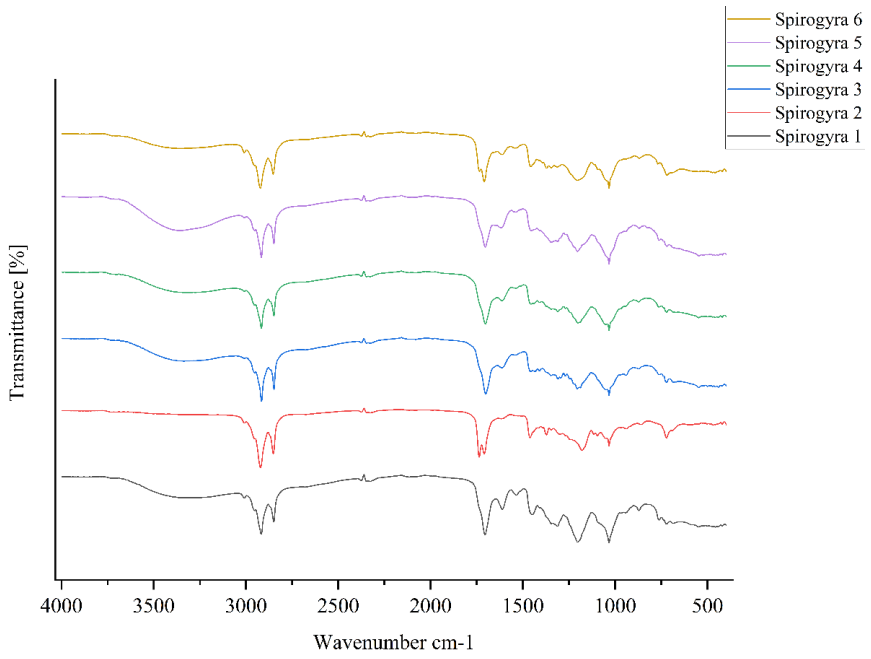

Figure 7 FTIR spectra analysis of SPE1-SPE6.

Conclusions

This study demonstrates that combining morphological, *rbc*L-based molecular, and chemical analyses provides a comprehensive framework for characterizing *Spirogyra* species from Sakon Nakhon province. It was identified by using morphology and molecular biology as *Spirogyra submaxima*, *S. fluviatilis*, *S. maxima*, and *S. chungkingensis*. The *rbc*L gene can be used to study species identification but must be studied in combination with morphology. Molecular biology studies can help distinguish species with similar morphological characteristics. LC-MS analysis of 6 *Spirogyra* samples detected 60 compounds in both positive and negative ionization modes, among which thirty compounds were consistently present across all 6 samples. However, each of the 6 *Spirogyra* also contained distinct compounds, representing specific variations of the algae found in different locations. The integration of these approaches allows the differentiation of closely related species and reveals

both shared and locality-specific metabolites. These findings suggest that chemical profiles may reflect environmental influences and species adaptation, offering insights into the ecological diversity of *Spirogyra*. Overall, this study establishes baseline knowledge that can guide future taxonomic, ecological, and biotechnological investigations, including the exploration of bioactive compounds for industrial applications.

Acknowledgements

This research was funded by the Thailand Science Research and Innovation (TSRI) and National Science, Research and Innovation (NSPF) or Fundamental Fund (FF) 2023, Sakon Nakhon Rajabhat University, Thailand.

Declaration of Generative AI in Scientific Writing

This manuscript used generative artificial intelligence (AI) tools, namely QuillBot for grammar checks. All scientific content, analysis, and conclusion were developed by authors.

CRediT Author Statement

Nopparut Sitthiwong: Conceptualization, Methodology, Supervision, Validation, Investigation, Funding acquisition, Project administration, Resources, and Writing –original draft. **Kaewkanlaya Sotthisawad**: Methodology, Data curation, Formal analysis, Investigation, Validation, Resources, and Visualization. **Supakorn Arthan**: Conceptualization, Resources, Methodology, Data curation, Validation, Investigation, Visualization Project Administration, Funding acquisition, and Writing – review & editing. **Jeeraporn Pekkoh**: Data curation, Formal analysis, Investigation, Validation, and Visualization. **Kittiya Phinyo**: Data curation, Formal analysis, Investigation, Validation, and Visualization.

References

[1] S Thiamdao and Y Peerapornpisal. Diversity of edible freshwater macroalgae in Mekong and Nan Rivers. *Journal of Fisheries Technology Research* 2009; **3(1)**, 115-124.

[2] S Nagabhushana and SG Malammanavar. The occurrence of genus *Spirogyra* (Zygnemataceae, Chlorophyceae) from the ponds of Shivamogga district and it's distributional additions to the algal flora of Karnataka, India. *International Journal of Botany Studies* 2021; **6(3)**, 103-115.

[3] C Permann, N Gierlinger and A Holzinger. Zygospore of the green alga *Spirogyra*: new insight from structural and chemical imaging. *Frontiers in Plant Science* 2022; **13**, 1080111.

[4] Y Peerapornpisal. *Freshwater algae in Thailand*. 3rd ed. Department of Biology, Faculty of Science, Chiang Mai University, Chiang Mai, 2015, p. 204-205.

[5] S Thiamdao and Y Peerapornpisal. Morphological observation of *Spirogyra elliosospora* Transeau, an edible freshwater macroalgae. *Journal of The Microscopy Society of Thailand* 2011; **4(2)**, 94-97.

[6] MD Guiry and GM Guiry. *Algaebase* - world-wide electronic publication, National University of Ireland, Galway, Available at: https://www.algaebase.org/search/genus/detail/?genus_id=43564, accessed September 2025.

[7] HA Berry and CA Lembi. Effect of temperature and irradiance on the seasonal variation of a *Spirogyra* (Chlorophyta) population in a Midwestern Lake (USA). *Journal of Phycology* 2000; **36**, 841-851.

[8] T Takano, S Higuchi, H Ikegaya, R Matsuzaki, M Kawachi, F Takahashi and H Nozaki. Identification of 13 *Spirogyra* species (Zygnemataceae) by traits of sexual reproduction induced under Laboratory culture conditions. *Scientific Reports* 2019; **9(1)**, 7458.

[9] P Wongsawad and Y Peerapornpisal. Molecular identification and phylogenetic relationship of green algae, *Spirogyra elliosospora* (Chlorophyta) using ISSR and *rbc*L markers. *Saudi Journal of Biological Sciences* 2014; **21**, 505-510.

[10] CS Drummond, J Hall, KG Karol, CF Delwiche and RM McCourt. Phylogeny of *Spirogyra* and *Sirogonium* (Zygnematophyceae) based on *rbc*L sequence DATA 1. *Journal of Phycology* 2005; **41(5)**, 1055-1064.

[11] B Yongkhamcha and N Buddhakala. Phytochemical compositions, nutritional contents, cytotoxicity and anti-inflammatory activity of different extracts from *Spirogyra neglecta* (Hassall) Kützing. *Trends in Sciences* 2023; **20(4)**, 6528.

[12] J Prarthana and KR Maruthi. Screening of phytochemicals & bioactive antibacterial activity in *Spirogyra* sp. *International Journal of Advanced Research* 2017; **5(7)**, 1145-1154.

[13] Z Shah, SL Badshah, A Iqbal, Z Shah, AH Emwas and M Jaremko. Investigation of important biochemical compounds from selected freshwater macroalgae and their role in agriculture. *Chemical and Biological Technologies in Agriculture* 2022; **9(1)**, 9.

[14] J Wizi, L Ni, WK Darkwah and L Xianglan. Analysis of bioactive compounds from different algae samples extracted with ultrasound: Characterization, phytochemical contents and antioxidant potentials. *Pharmacognosy Research* 2022; **14(1)**, 35-44.

[15] S Nagabhushana, ASK Yohannan, SG Malammanavar, A Raman and G Packiaraj. Phytochemical constituents and bio-potentiality of *Spirogyra porticalis* (O.F. Müller) Dumortier from the perennial pond of Karnataka, India. *Notulae Scientia Biologicae* 2025; **17(2)**, 12300-12300.

[16] N Sitthiwong. Pigment and nutritional value of *Spirogyra* spp. in Sakon Nakhon, Nakhon Phanom and Mukdahan Provinces. *Progress in Applied Science and Technology* 2019; **9(1)**, 10-21.

[17] N Sitthiwong, J Sumangka, S Michaitrakun and K Sotthisawad. Total phenolic compound and antimicrobial activity of *Spirogyra* spp. *Progress in Applied Science and Technology* 2024; **14(1)**, 65-72.

[18] DM John, BA Whitton and AJ Brook. *The freshwater algal flora of the british isles: An identification guide to freshwater and terrestrial algae.* 2nd ed. Cambridge University Press, Cambridge, 2011, p. 587-602.

[19] R Stancheva, JD Hall, RM McCourt and RG Sheath. Identity and phylogenetic placement of *Spirogyra* species (Zygnematophyceae, Charophyta) from California streams and elsewhere. *Journal of Phycology* 2013; **49**, 588-607.

[20] P Wilkie, AD Poulsen, D Harris and LL Forrest. The collection and storage of plant material for DNA extraction: the teabag method. *Gardens' Bulletin Singapore* 2013; **65(2)**, 231-234.

[21] S Arthan, J Jandaruang and K Namwongsa. Screening of antioxidant, anti-tyrosinase, antibacterial, alpha-glucosidase inhibitory activities and chemical profile from roots of *Indigofera suffruticosa*. *Moroccan Journal of Chemistry* 2025; **13(3)**, 1442-1460.

[22] EI Abdel-Aal, AM Haroon and J Mofeed. Successive solvent extraction and GC - MS analysis for the evaluation of the phytochemical constituents of the filamentous green alga *Spirogyra longata*. *The Egyptian Journal of Aquatic Research* 2015; **4(3)**, 233-246.

[23] J Kumar, D Priyanka, AB Tayade, D Gupta, O Chaurasia, DK Upreti, K Toppo, R Arora, MR Suseela and RB Srivastava. Chemical composition and biological activities of trans-Himalayan alga *Spirogyra porticalis* (Muell.) Cleve. *PloS One* 2015; **10(2)**, e0118255.

[24] DH Mohammed and MA Al-katib. Active and phenolic compounds in *Spirogyra* sp. PDNA1 is an antibiotic for some bacteria and fungi. *Al-Kitab Journal for Pure Sciences* 2023; **7(1)**, 100-113.

[25] J Sun, Y Song, J Zhang, Z Huang, H Huo, J Zheng, Q Zhang, Y Zhao, J Li and P Tu. Characterization and quantitative analysis of phenylpropanoid amides in eggplant (*Solanum melongena* L.) by high performance liquid chromatography coupled with diode array detection and hybrid ion trap time-of-flight mass spectrometry. *Journal of Agricultural and Food Chemistry* 2015; **63(13)**, 3426-3436.

[26] AR Sherwood, JM Neumann, M Dittbern-Wang and KY Conklin. Diversity of the green algal *Spirogyra* (Conjugatophyceae) in the Hawaiian Islands. *Phycologia* 2018; **57(3)**, 331-344.

[27] P Wongsawad and Y Peerapornpisal. Morphological and molecular profiling of *Spirogyra* from northeastern and northern Thailand using inter simple sequence repeat (ISSR) markers. *Saudi Journal of Biological Sciences* 2015; **22(4)**, 382-389.

[28] M El-Sheekh, M Schagerl, M Gharieb and GA Elsoud. Induction of sexual reproduction and zygospore patterns in the filamentous green alga *Spirogyra* link (Conjugatophyceae: Zygnematales). *Journal of BioScience and Biotechnology* 2017; **6(2)**, 147-154.

[29] K Phinyo, K Saeku, W Nunto, J Pekkoh and T Prasertsin. Morphological and molecular characterization of *Spirogyra* species from water bodies in Chiang Rai Province, Thailand: Insights into bioactivity and antioxidant potential. *Sains Malaysiana* 2024; **53(5)**, 1093-1104.

[30] P Wongsawad and Y Peerapornpisal. Ecological relevance and physical morphology of green algae, *Spirogyra* sp. In northern Thailand. *Journal of Yala Rajabhat University* 2013; **8(1)**, 1-8.

[31] R Hainz, C Wober and M Schagerl. The relationship between *Spirogyra* (Zygnematophyceae, Streptophyta) filament type groups and environmental conditions in Central Europe. *Aquatic Botany* 2009; **91(3)**, 173-180.

[32] S Sriwattana, N Chokumnoyporn and C Brennan. Chemical composition and sensory profile of *Spirogyra neglecta* (Hassall) Kützing. *International Journal of Food Science and Technology* 2024; **59(12)**, 9336-9344.

[33] MN Khalid and M Shameel. Studies on the phycochemistry and biological activity of *Spirogyra rhizoides* (Chlorophycota). *Pakistan Journal of Botany* 2012; **44(5)**, 1815-1820.

[34] A Juneja, RM Ceballos and GS Murthy. Effects of environmental factors and nutrient availability on the biochemical composition of algae for biofuels production: A review. *Energies* 2013; **6(9)**, 4607-4638.

[35] C Lopes, JMC Obando, TCD Santos, DN Cavalcanti and VL Teixeira. Abiotic factors modulating metabolite composition in brown algae (Phaeophyceae): Ecological impacts and opportunities for bioprospecting of bioactive compounds. *Marine Drugs* 2024; **22(12)**, 544.

[36] Y Zhao, J Zhou, L Chen, S Li, Y Yin, A Jeyaraj, S Liu, J Zhuang, Y Wang, X Chen and X Li. Allelopathic effect of *Osmanthus fragrans* changes the soil microbial community and increases the soil nutrients and the aroma quality of tea leaves. *Journal of Agricultural and Food Chemistry* 2025; **73(22)**, 13818-13831.

[37] RZ Mehrizi, AF Bafghi, N Vahid, MRS Ardakani, MN Meybodi and H Zare-Zardini. Evaluation of the anti-Leishmanial activity of the hydroalcoholic extract of green algae (*Spirogyra*): Investigation of weight indicators (lesion size and organ weights) in BALB/c Mice. *Acta Parasitologica* 2025; **70(1)**, 51.

[38] B Ghazala and M Shameel. Phytochemistry and bioactivity of some freshwater green algae from Pakistan. *Pharmaceutical Biology* 2008; **43(4)**, 358-369.

[39] I Ahmad, FM Sarim, B Ullah, R Ullah and T Sageretia. Phytotoxic and cytotoxic activities of 3 species of *Spirogyra*. *Pakistan Journal of Plant Sciences* 2012; **18(1)**, 69-72.

[40] Z Djezzar, A Aidi, H Rehali, S Ziad and T Othmane. Characterization of activated carbon produced from the green algae *Spirogyra* used as a cost-effective adsorbent for enhanced removal of copper (ii): Application in industrial wastewater treatment. *RSC Advances* 2024; **14(8)**, 5276-5289.

[41] A Mansoori, N Singh, SK Dubey, TK Thakur, N Alkan, SN Das and A Kumar. Phytochemical characterization and assessment of crude extracts from *Lantana camara* L. for antioxidant and antimicrobial activity. *Frontiers in Agronomy* 2020; **2**, 582268.